electronic reprint

STRUCTURAL CHEMISTRY

ISSN: 2053-2296
journals.iucr.org/c

# *Syn*- and *anti*-rotamers of the *ortho*-stereoisomer $[Pt\{(o\text{-}BrC_6F_4)N(CH_2)_2NEt_2\}Cl(py)]$

**Ruchika Ojha, Alan M. Bond, Peter C. Junk and Glen B. Deacon**

*Acta Cryst.* (2025). C**81**, 513–518

STRUCTURAL CHEMISTRY

ISSN 2053-2296

# *Syn*- and *anti*-rotamers of the *ortho*-stereoisomer [Pt{($o$-BrC$_6$F$_4$)N(CH$_2$)$_2$NEt$_2$}Cl(py)]

**Ruchika Ojha,[a,b] Alan M. Bond,[a]* Peter C. Junk[c]* and Glen B. Deacon[a]***

[a]School of Chemistry, Monash University, VIC 3800, Australia, [b]School of Science, STEM College, RMIT University, Melbourne, VIC 3000, Australia, and [c]College of Science & Engineering, James Cook University, Townsville, Qld 4811, Australia. *Correspondence e-mail: alan.bond@monash.edu, peter.junk@jcu.edu.au, glen.deacon@monash.edu

Received 23 July 2025
Accepted 30 July 2025

Edited by M. Yousufuddin, University of North Texas at Dallas, USA

**Keywords:** crystal structure; platinum anticancer agent; *syn* and *anti* rotamers; agostic interactions; synchrotron.

**CCDC references:** 2481234; 2477306

**Supporting information:** this article has supporting information at journals.iucr.org/c

The crystal structure of the *ortho*-isomer *trans*-[*N*-(2-bromo-3,4,5,6-tetrafluorophenyl)-*N*′,*N*′-diethylethane-1,2-diaminato(1−)]chloridopyridineplatinum(II), [PtBr$_{0.1}$(C$_{12}$H$_{14}$BrF$_4$N$_2$)Cl$_{0.9}$(C$_5$H$_5$N)][PtBr$_{0.4}$(C$_{12}$H$_{14}$BrF$_4$N$_2$)Cl$_{0.6}$(C$_5$H$_5$N)] or [Pt{($o$-BrC$_6$F$_4$)N(CH$_2$)$_2$NEt$_2$}Cl(py)], **1*o***, revealed *syn* and *anti* rotamers in a 1:1 ratio in the solid state. **1*o*** crystallizes in the centrosymmetric space group $P\overline{1}$. The Pt-coordinated Cl ligand exhibits partial occupancy with Br, predominantly in the *syn*-rotamer. Notably, agostic interactions are observed between the Pt centre and a H atom of one of the ethyl groups. The *ortho*-isomer **1*o*** was successfully isolated as a side product from the reaction of [Pt{H$_2$N(CH$_2$)$_2$NEt$_2$}Cl$_2$], Tl$_2$CO$_3$ and C$_6$F$_5$Br. While the *para*-isomer [Pt{($p$-BrC$_6$F$_4$)N(CH$_2$)$_2$NEt$_2$}Cl(py)], **1*p***, is the main product, the higher solubility of **1*o*** facilitates its isolation.

## 1. Introduction

Polyfluoroaryl-substituted organoamidoplatinum(II) complexes [Pt{*R*N(CH$_2$)$_2$N*R*′$_2$}*X*(py)] [*R* = *p*-*Y*C$_6$F$_4$ (*Y* = F, Cl, Br or I), CH$_3$, *etc*.; *R*′ = Me or Et; *X* = Cl, Br or I; py = pyridine] have been shown to have good *in vitro* and modest *in vivo* activity (Talarico *et al.*, 1999; Ojha *et al.*, 2021) against a number of tumour cells. They are conveniently prepared by reaction of [Pt*X*$_2$(NH$_2$CH$_2$CH$_2$N*R*′$_2$)] with thallium(I) carbonate (or K$_2$CO$_3$ in some cases) and a polyfluoroarene, *R*F, in boiling pyridine (Fig. 1) (Battle *et al.*, 2010; Ojha *et al.*, 2015). The CO$_2$ generated from Tl$_2$CO$_3$ during the reaction was trapped as BaCO$_3$ by a Ba(OH)$_2$ solution, and the yield of CO$_2$ was measured gravimetrically.

One step in the complex CO$_2$ elimination reaction paths is nucleophilic substitution of F on the polyfluorobenzene, *R*F, by the –NH$_2$ group, plausibly partially deprotonated by the carbonate group. The substitution pattern of the major products (Battle *et al.*, 2010; Buxton *et al.*, 1988; Deacon *et al.*, 1991) corresponds to that (*para* to substituent *Y*), as observed in the nucleophilic substitution of polyfluoroarenes (Chambers *et al.*, 1974, 1977; Chambers, 2004). Although the $^{19}$F NMR spectra of crude reaction products sometimes suggested that the reactions were not entirely regiospecific, simple recrystallization usually gave isomerically pure products (Battle *et al.*, 2010; Buxton *et al.*, 1988; Deacon *et al.*, 1991). However, the reaction of [PtCl$_2$(en)] (en is ethylenediamine), Tl$_2$CO$_3$ and 2-bromo-1,3,4,5-tetrafluorobenzene in pyridine gave isomers with the N atom *para* to both H and Br. Only the former was isolated, the latter being identified spectroscopically in the reaction mixture (Battle *et al.*, 2010).

We have recently reported anticancer activity (Ojha *et al.*, 2021), chemical oxidation (Ojha *et al.*, 2023) and the synthesis

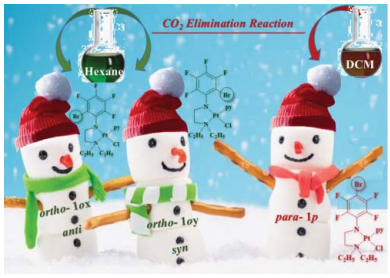

of [Pt{($p$-BrC$_6$F$_4$)N(CH$_2$)$_2$NEt$_2$}Cl(py)], **1*p*** (with $X$ = Cl, $R'$ = Et and $R$ = $p$-BrC$_6$F$_4$), in 64% yield by reaction between [PtCl$_2${H$_2$N(CH$_2$)$_2$NEt$_2$}], Tl$_2$CO$_3$ and C$_6$F$_5$Br in pyridine (Fig. 2) (Ojha *et al.*, 2015). During this study, it was noticed that the hexane washings of the crude product (to remove adherent pyridine) had a yellow colour. We have now investigated the source of the colour and have isolated and crystallized the *ortho*-isomer, [Pt{($o$-BrC$_6$F$_4$)N(CH$_2$)$_2$NEt$_2$}Cl(py)], **1*o***. This has been identified by X-ray crystallography, employing synchrotron radiation, and found to crystallize as a 1:1 mixture of the *syn* (**1*ox***) and *anti* (**1*oy*)** rotamers (with respect to the $o$-Br and Pt—Cl positions) in the asymmetric unit.

## 2. Experimental

### 2.1. General

NMR spectra were recorded in deuterated acetone with a Bruker DPX 400 spectrometer supported by *Top Spin* NMR software on a Windows NT workstation. CFCl$_3$ and tetramethylsilane (TMS) were used for the internal calibration of the $^{19}$F NMR and $^{1}$H NMR spectra, respectively. IR spectra were recorded on a Perkin–Elmer 1600 FT–IR spectrophotometer as Nujol and hexachlorobutadiene (HCB) mulls between NaCl plates or recorded with an Agilent Cary 630 attenuated total reflectance (ATR) spectrometer in the range 4000–600 cm$^{-1}$.

### 2.2. X-ray crystallography

Crystal data, data collection and structure refinement details are summarized in Table 1. X-ray diffraction data obtained from single crystals of **1*ox***/**1*oy*** were collected at a wavelength of $\lambda$ = 0.712 Å using the MX1 beamline at the Australian Synchrotron, Victoria, Australia, with a *Blue Ice* (McPhillips *et al.*, 2002) GUI, using the same method as mentioned in the *Experimental* section of Ojha *et al.* (2015). Data were processed with the *XDS* (Kabsch, 1993) software package. Single crystals were loaded onto a fine glass fiber or cryoloop using hydrocarbon oil, with the collection kept at 123 K using an Oxford Cryosystems open-flow N$_2$ Cryostream. The program *OLEX2* (Dolomanov *et al.*, 2009) was used as the graphical interface. H atoms attached to C atoms were placed in calculated positions and allowed to ride on the atom to which they were attached.

**Table 1**
Crystallographic data for the molecular structures of **1*ox***/**1*oy*** and comparison with **1*p***.

| | *ortho*-**1*ox***/**1*oy*** | **1*p*** (Ojha *et al.*, 2015) |
|---|---|---|
| Empirical formula | C$_{34}$H$_{38}$Br$_{2.5}$Cl$_{1.5}$F$_8$N$_6$Pt$_2$ | C$_{17}$H$_{19}$BrClF$_4$N$_3$Pt |
| Formula weight | 1321.39 | 651.78 |
| Crystal system | Triclinic | Monoclinic |
| Space group | $P\overline{1}$ | $P2_1/c$ |
| $a$ (Å) | 9.4810 (19) | 10.960 (2) |
| $b$ (Å) | 14.656 (3) | 11.961 (2) |
| $c$ (Å) | 15.094 (3) | 15.224 (3) |
| $\alpha$ (°) | 75.02 (3) | 90 |
| $\beta$ (°) | 74.62 (3) | 98.46 (3) |
| $\gamma$ (°) | 86.28 (3) | 90 |
| $V$ (Å$^3$) | 1953.5 (8) | 1974.0 (7) |
| $Z$ | 2 | 4 |
| $\rho$ (calcd) (Mg m$^{-3}$) | 2.246 | 2.193 |
| $\mu$ (mm$^{-1}$) | 9.790 | 9.311 |
| $F$(000) | 1246.0 | 1232 |
| Reflections collected/unique | 24773/8572 | 22718/3354 |
| $R_{int}$ | 0.0553 | 0.0267 |
| $2\theta_{max}$ (°) | 55.8 | 50.0 |
| Goodness-of-fit on $F^2$ | 1.052 | 1.126 |
| $R1$ indices [$I > 2\sigma(I)$] | 0.0626 | 0.0217 |
| $wR2$ indices | 0.1743 | 0.0518 |

Computer programs: *Blue Ice* (McPhillips *et al.*, 2002), *XDS* (Kabsch, 1993), *SHELXT2014* (Sheldrick, 2015*a*) and *SHELXL2018* (Sheldrick, 2015*b*).

### 2.3. Isolation of *ortho*-isomers [Pt{($o$-BrC$_6$F$_4$)NCH$_2$CH$_2$NEt$_2$}Cl(py)], 1*ox*/1*oy*

After completion of the typical synthesis of **1*p*** by a CO$_2$ elimination reaction (Ojha *et al.*, 2015), pyridine was removed under vacuum until dryness. Hexane was added to remove traces of residual pyridine and decanted. The major product **1*p*** was extracted with acetone from the remaining solid, as reported earlier. The decanted hexane was yellow–orange, rather than colourless, indicating that it had not just removed the remaining pyridine, but possibly an isomer.

To isolate and crystallize the isomers, some acetone was added to the decanted solution. Crystals of **1*ox***/**1*oy*** suitable for structure determination were obtained by slow evaporation of the solvent. **1*ox*** and **1*oy*** are present in a 1:1 ratio. Apart from the X-ray data, the integrations for $^{1}$H resonances measured in (CD$_3$)$_2$CO show **1*ox***/**1*oy*** in a 1:1 ratio.

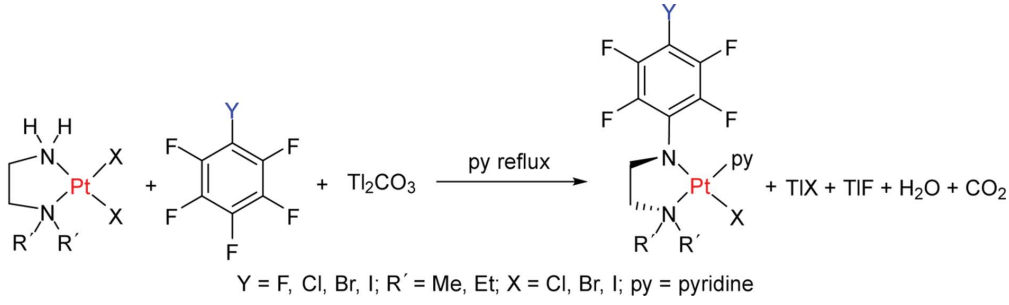


**Figure 1**
General synthesis of [Pt{$R$N(CH$_2$)$_2$N$R'_2$}$X$(py)].

**Table 2**
Observed and calculated chemical shifts (ppm) for **1*o*** and their comparison with calculated *m*-$BrC_6F_4$ organoamidoplatinum(II) compounds.

| F | Observed | Calculated for *o*-$BrC_6F_4$ | F | Calculated for *m*-$BrC_6F_4$ |
|---|---|---|---|---|
| F3 | −140.6 | −140.6 | F2 | −122.5 |
| F6 | −151.2 | −151.1 | F6 | −145.1 |
| F5 | −160.9 | −163.2 | F4 | −145.2 |
| F4 | −171.1 | −174.8 | F5 | −169.2 |

Metallic yellow–orange blocks (yield: 0.130 g, 20%). $^{19}$F NMR [$(CD_3)_2CO$]: $\delta$ −140.6 (*d*, 2F, F3), −151.2 (*d*, 2F, F6), −160.9 (*t*, 2F, F5), −171.1 (*m*, 2F, F4). $^1$H NMR [$(CD_3)_2CO$]: $\delta$ 1.53 (*t*, $^3J_{H,H}$ = 7.15 Hz, 12H, $NCH_2C\mathbf{H_3}$), 2.48 (*t*, with $^{195}$Pt–H satellites, $^3J_{H,H}$ = 6, $^3J_{H,Pt}$ = 30 Hz, 4H, $C\mathbf{H_2}NEt_2$), 2.80 (*m*, 4H, NC**HA**HB$CH_3$), 3.34 [*m*, 8H, made up of 4H $C\mathbf{H_2}N$(*p*-$BrC_6F_4$) and 4H NC**HB**HA$CH_3$], 7.09 [*t*, $^3J_{H,H}$ = 7 Hz, 2H, **H3,5**(py)], 7.15 [*t*, 2H, $^3J_{H,H}$ = 7 Hz, **H3,5**(py)], 7.65 [*tt*, $^3J_{H,H}$ = 7, $^4J_{H,H}$ = 1 Hz, 1H, **H4** (py)], 7.70 [*tt*, $^3J_{H,H}$ = 7, $^4J_{H,H}$ = 1 Hz, 1H, **H4** (py)], 8.50 [*d* with $^{195}$Pt–H satellites, $^3J_{H,H}$ = 5, $^3J_{H,Pt}$ = 36 Hz, 2H, **H2,6**(py)], 8.54 [*d* with $^{195}$Pt–H satellites, $^3J_{H,H}$ = 5, $^3J_{H,Pt}$ = 36 Hz, 2H, **H2,6**(py)]. IR (cm$^{-1}$): 2960 (*w*), 2922 (*w*), 2853 (*w*), 1654 (*w*), 1618 (*w*), 1607 (*b*), 1458 (*s*), 1450 (*s*), 1375 (*m*), 1345 (*w*), 1258 (*s*), 1208 (*m*), 1133 (*s*), 1073 (*s*), 1014 (*s*), 962 (*s*), 898 (*m*), 875 (*m*), 794 (*s*), 765 (*s*), 691 (*s*).

## 3. Results and discussion

The *ortho*-isomer **1*o*** was preferentially isolated due to its markedly greater solubility in hexane compared to the *para*-isomer **1*p***. The synthesis predominantly afforded **1*p*** (Ojha *et al.*, 2015) by a $CO_2$ elimination reaction (Fig. 2). A subsequent hexane washing, intended to remove residual pyridine, unexpectedly exhibited a yellow–orange coloration. This observation suggested the presence of an additional platinum-containing species, which could be a different isomer, rather than merely solvent. Therefore, it was investigated further, and slow evaporation of the hexane washing enabled the isolation of the *ortho*-isomer [Pt{(*o*-$BrC_6F_4$)$NCH_2CH_2NEt_2$}-Cl(py)], **1*o***, which was considerably more soluble in the low-polarity solvent hexane (with a trace of pyridine) than **1*p***. The *ortho*-isomer **1*o*** crystallized as a 1:1 mixture of the *anti* (**1*ox***) and *syn* (**1*oy***) rotamers in the asymmetric unit. This procedure facilitates isolation of the pure *para*-isomer (**1*p***) as the major product from the reaction mixture.

### 3.1. Characterization of 1*o*

The initial identification of **1*o*** was *via* $^1$H and $^{19}$F NMR spectroscopy in $(CD_3)_2CO$. The coordination of pyridine and the amide ligand to platinum was evident from the observation of $^3J(^{195}Pt,H)$ satellites ($^{195}$Pt isotope, nuclear spin $I$ = 1/2, natural abundance = 33.8%) on the signals of the H2,6(pyridine) and $CH_2$(N-ethyl) protons, with the coupling constants $^3J$(Pt,H2,6-py) and $^3J$(Pt,$CH_2$-N) having values (36 and 30 Hz, respectively) similar to those (35 and 28 Hz) observed for **1*p*** (Ojha *et al.*, 2015). Other $^1$H chemical shifts and integrations, which are similar to those of **1*p***, are consistent with the composition of **1*o***.

Evidence for the proposed polyfluorophenyl substitution pattern comes from $^{19}$F NMR spectroscopy. Four equal-intensity $^{19}$F resonances indicate either a *m*-$BrC_6F_4$ or an *o*-$BrC_6F_4$ group compared with two for **1*p*** (Fig. S1 for the F-atom numbering system). Chemical shift calculations {based on substituent chemical shifts for Br (Bruce, 1968; Ando & Matsuura, 1995), for *o*- and *m*-[N(–$CH_2$)Pt] groups derived from **1*p*** (Ojha *et al.*, 2015), and for *p*-[N($CH_2$–)Pt] derived from several [Pt{$C_6F_5NCH_2CH_2NEt_2$}*X*(py)] complexes (Deacon *et al.*, 1991)] clearly support the presence of an *o*-$BrC_6F_4$ substituent in **1*o***, and compares well with the observed chemical shift (Table 2). The $^{19}$F NMR spectrum is provided in the supporting information (Fig. S2) and shows the same chemical shifts for **1*ox*** and **1*oy***. In the $^1$H NMR spectrum, the pyridine resonances in **1*ox*** and **1*oy*** appear 0.1 ppm apart, as shown in Fig. S3, and show **1*ox*** and **1*oy*** in a 1:1 ratio.

The unequivocal identification of **1*o*** was provided by X-ray crystallography. The crystallographic data differ considerably from those of **1*p*** (Table 1). **1*o*** crystallizes in the triclinic space

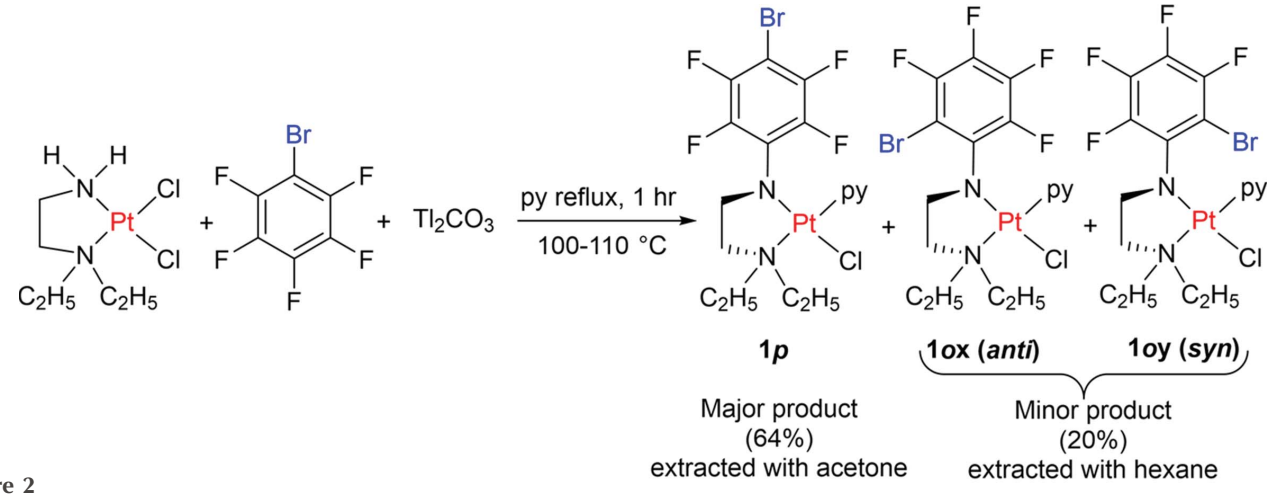


**Figure 2**
Carbon dioxide elimination reaction for the synthesis of **1*p*** and **1*ox***/**1*oy***.

**Table 3**
Selected bond lengths (Å) and bond angles (°) for **1*ox***/**1*oy*** and comparison with **1*p***.

| Bond | **1*ox*** | **1*oy*** | **1*p*** | Angle | **1*ox*** | **1*oy*** | **1*p*** |
|---|---|---|---|---|---|---|---|
| Pt—Cl | 2.35 (3) | 2.323 (7) | 2.344 (10) | Cl—Pt—N(amide) | 177.5 (9) | 175.8 (4) | 176.17 (9) |
| Pt—Br | 2.534 (16) | 2.62 (3) | – | N(amide)—Pt—N($Et_2$) | 84.2 (4) | 83.5 (4) | 82.65 (12) |
| Pt—N(amide) | 1.993 (11) | 2.006 (11) | 2.006 (3) | N(amide)—Pt—N(py) | 91.6 (4) | 93.2 (4) | 93.27 (12) |
| Pt—N($Et_2$) | 2.087 (10) | 2.076 (9) | 2.074 (3) | Cl—Pt—N($Et_2$) | 93.3 (8) | 92.3 (4) | 93.98 (9) |
| Pt—N(py) | 2.034 (9) | 2.026 (9) | 2.013 (3) | Cl—Pt—N(py) | 90.9 (8) | 90.9 (4) | 90.25 (8) |
| N(amide)—C($C_6F_4$) | 1.383 (19) | 1.362 (19) | 1.354 (4) | N($Et_2$)—Pt—N(py) | 174.8 (4) | 173.8 (4) | 173.53 (12) |

group $P\bar{1}$ with the rotamers **1*ox*** and **1*oy*** (Fig. 2) in the asymmetric unit (Table 1). In **1*ox***, Br and Cl are *anti* with a Br—Pt—Cl angle of 156.86 (6)°, whereas in **1*oy***, they are in a *syn* disposition with a Br—Pt—Cl angle of 113.61 (8)°.

In the proposed mechanism, initially, both chloride ligands on Pt are replaced by pyridine. Due to the hydrogen bonding between –$NH_2$ and $CO_3^{2-}$, a lone-pair character is generated on the N atom and initiates nucleophilic substitution in the polyfluoroaryl ring (Deacon *et al.*, 1998), as shown in Scheme S1 in the supporting information.

The Meisenheimer intermediates involved in the formation of **1*p*** and **1*o*** are depicted in Fig. 3. In the case of **1*p***, the negative charge generated during the nucleophilic substitution of the polyfluoroaryl ring is stabilized by two *ortho*- and two *meta*-fluorines, relative to the site of substitution (see Scheme S2 in the supporting information). Similarly, the formation of the *ortho*-Br isomers is also feasible because the negative charge in the Meisenheimer intermediate (Fig. 3) is located *para* and *ortho* to the site of substitution. This causes the positions *ortho* and *para* to Br to be electron deficient and thus susceptible to nucleophilic attack (Scheme S2). The negative charge in the Meisenheimer intermediate is stabilized by two *o*-F and two *m*-F atoms in **1*p***, and by two *o*-F and one *m*-F atom in **1*o***.

The displacement of the pyridine ligand *trans* to the amide group by the chloride ion gives the target compound (see Scheme S1 in the supporting information). This regiospecificity is obtained as the *trans* effect of the –N(*p*-$BrC_6F_4$) N atom is greater than that of the –$NEt_2$ N atom, in line with the *trans*-influence values from platinum–H coupling constants (Buxton *et al.*, 1988).

In **1*ox***, the Cl ligand coordinated to the Pt atom has a shared occupancy with Br, *cf.* 0.59 (1):0.41 (1), yielding 0.59 Cl and 0.41 Br, while for **1*oy***, the Cl remains the major occupant, with 0.91 (1) Cl and a slight sharing 0.09 (1) with Br. The Br atom is derived from $C_6F_5Br$. It has previously been shown that some elimination of Br occurs during the oxidation of **1*p*** by hydrogen peroxide (Ojha *et al.*, 2021), and replacement of chloride coordinated to Pt by bromide is consistent with the stability constants for soft metals (Ault *et al.*, 1977).

The molecular structure of **1*o*** shows that the Pt atom is coordinated in a square-planar array by a chelating {(*o*-Br-$C_6F_4$)$NCH_2CH_2NEt_2$}$^-$, pyridine and chloride ligands, with the chloride ligand being *trans* to the amide N atom and pyridine being *trans* to the amine group (Fig. 4). Thus, it is a *trans*-isomer in terms of the positions of the like-charged donor atoms. Selected bond lengths and angles for **1*ox***/**1*oy*** are given in Table 3 and compared with those of **1*p***. In general, the values for **1*ox***/**1*oy*** and **1*p*** agree within or near the 3 e.s.d. level. However, the Pt—Cl bond of **1*ox*** is longer than that of **1*oy*** or **1*p***, owing to the shared Cl/Br occupancy. This is not a steric effect as the bond does not appear crowded. Supramolecular effects need to be considered. The Pt—N bond lengths follow the sequence Pt—N(amide) < Pt—N(py) < Pt—N($Et_2$) (Table 3), as was also observed for **1*p***. Most bond angles around the Pt centre are 90°, with the smallest being the bite angles of 84.1° for **1*ox*** and 83.5° for **1*oy***. The –$NCH_2$—$CH_2N$– sawhorse backbone is crooked, as seen in **1*p*** and other compounds of this class (Deacon *et al.*, 1991; Ojha *et al.*, 2016).

Intramolecular hydrogen bonding in **1*ox*** is observed as ($NEt_2$)H···Br, with an H···Br distance of 2.91 (2) Å, while

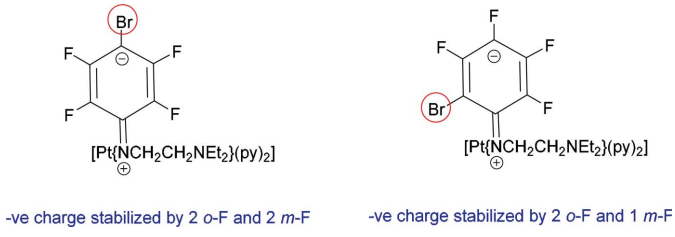


**Figure 3**
The Meisenheimer intermediates formed during the formation of **1*p*** (left) and **1*o*** (right).

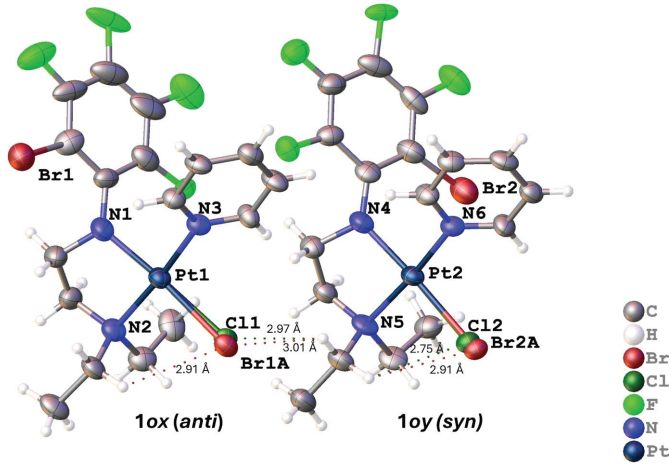


**Figure 4**
The molecular crystal structures of rotamers **1*ox*** (*anti*) and **1*oy*** (*syn*) cocrystallized in a single unit cell, showing 50% probability displacement ellipsoids.

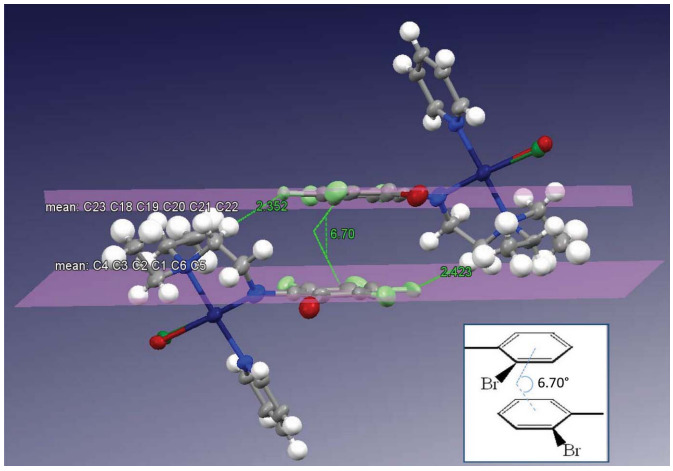


**Figure 5**
The $\pi$–$\pi$ interaction between the two polyfluoroaryl rings of two molecules with an angle of 6.703 (3)°, where the mirror image is rotated by 180° and the symmetry code is $(-x+1, -y, -z+1)$. The inset shows the *ortho*-Br atoms.

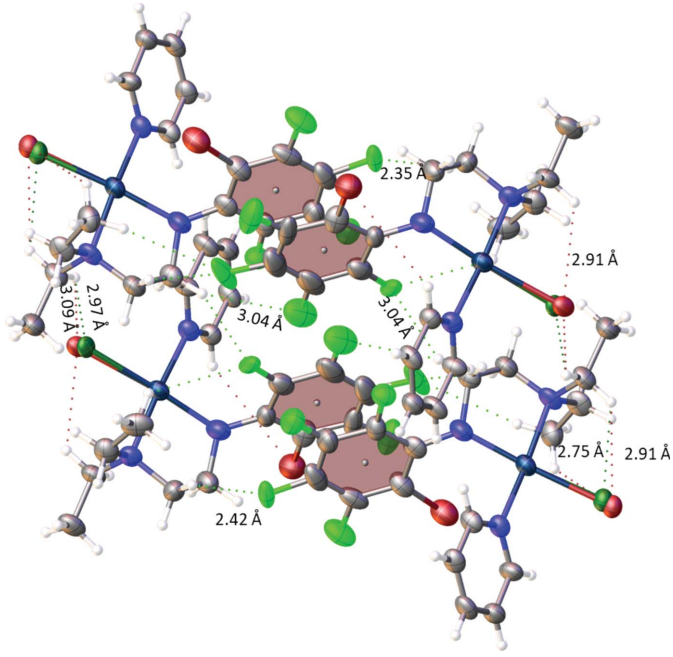


**Figure 6**
The crystal packing in **1*ox***/**1*oy***, showing the $\pi$–$\pi$ interactions between the two polyfluoroaryl rings of **1*ox*** and **1*oy***, and inter- and intramolecular hydrogen bonding.

**1*oy*** displayed an $(NEt_2)H\cdots Br$ interaction of 2.91 (4) Å and an $(NEt_2)H\cdots Cl$ interaction of 2.754 (9) Å (Fig. 4). Intermolecular hydrogen bonding between the **1*ox*** Cl/Br atoms and the $H(NEt_2)$ atom of **1*oy***, with an $(NEt_2)H\cdots Br$ distance of 3.093 (19) Å and an $(NEt_2)H\cdots Cl$ distance of 2.97 (3) Å, was also observed. A $\pi$–$\pi$ interaction between the two polyfluoroaryl rings is present (but not between py rings) and, in this arrangement, the polyfluoroaryl rings are not parallel but have an interplanar angle of 6.703 (3)°, as shown in Fig. 5. The *ortho*-Br atoms of both molecules are on the same side (as shown in the inset of Fig. 5), resulting in significant steric hindrance on one side. Consequently, the polyfluoroaryl rings are tilted at an angle of 6.703 (3)° to reduce the steric hindrance. The inter-centroid distance is 3.7969 (10) Å and the rings are offset by 1.7513 (15) Å, as was also observed for other similar compounds (Ojha *et al.*, 2018). On the other hand, in **1*p***, a $\pi$–$\pi$ interaction was observed between two pyridine rings, and not between polyfluoroaryl rings.

The $\pi$–$\pi$ interaction is further anchored by strong intermolecular hydrogen bonding between the *para*-F atom of **1*ox*** with a methylene H of the ligand backbone of **1*oy***, and *vice*

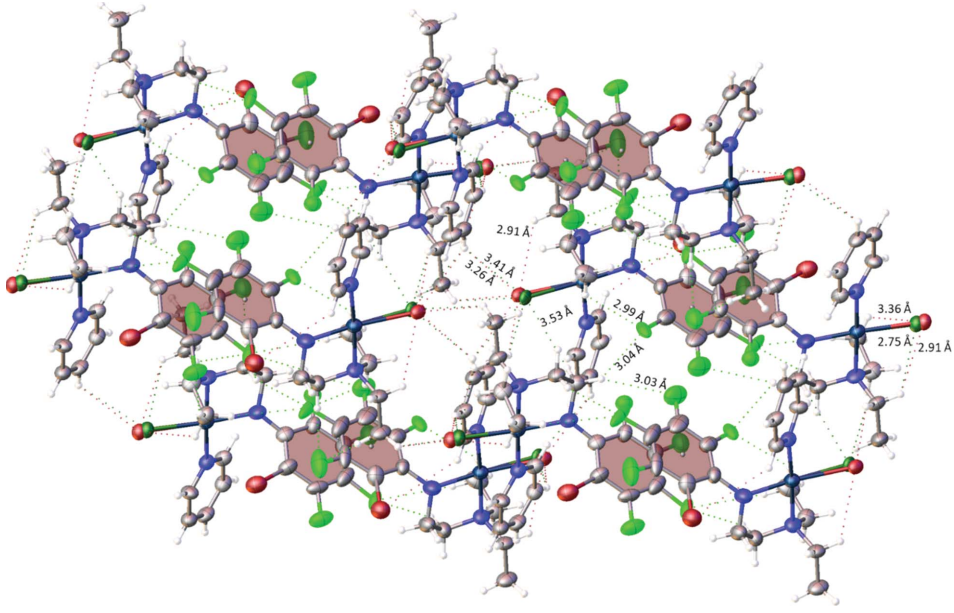


**Figure 7**
The crystal packing in **1*ox***/**1*oy***, showing $H\cdots Cl$ interactions for **1*ox*** and $C\cdots H$ interactions for **1*oy*** as intermolecular hydrogen bonding.

*versa*, as shown in Fig. 6, with H···F distances of 2.352 (7) and 2.424 (10) Å. Additionally, comparatively weak interactions, such as between the *para*-F atom of **1*ox*** with a methyl H atom of the $NEt_2$ group, with an H···F distance of 3.012 (8) Å, and a very weak interaction between the *ortho*-F atom of **1*ox*** and a methylene H atom of the ligand backbone of **1*oy***, with a H···F distance of 3.353 (11) Å, further stabilize the $\pi$–$\pi$ interaction.

In the **1*ox***/**1*oy*** isomers, one Et group makes an agostic interaction with Pt; the Pt···H($CH_3$) distance is 2.8043 (11) Å and the bond angles are 118.8 (3)° for H—Pt—N(py), 103.8 (3)° for H—Pt—N($C_6F_5$) and 65.3 (3)° for H—Pt—N$(Et)_2$ in **1*ox***, and the Pt···H($CH_3$) distance is 3.0032 (11) Å and the bond angles are 120.0 (3)° for H—Pt—N(py), 106.7 (3)° for H—Pt—N($C_6F_5$) and 66.1 (3)° for H—Pt—N$(Et)_2$ in **1*oy***. The *ortho*-F atom of **1*ox*** makes an intramolecular hydrogen-bonding contact with a methyl H atom of –N$(Et_2)$, which exhibits an agostic interaction with Pt, with an H···F distance of 2.994 (7) Å (Fig. 7). These rotamers display the entire network of supramolecular interactions, as illustrated in Fig. 7. The *p*-H(py) atom of **1*ox*** is anchored by intermolecular hydrogen bonding with the Cl/Br atom of the two adjacent **1*ox*** molecules, with H···Br distances of 3.050 (16) and 3.26 (2) Å, and H···Cl distances of 3.15 (2) and 3.41 (3) Å (see Fig. 7). Similarly, the *m*-H(py) atom is involved in hydrogen bonding with the Cl/Br atom of another **1*ox*** molecule, with a H···Br distance of 2.78 (4) Å and a H···Cl distance of 2.578 (8) Å.

Intermolecular F···H hydrogen bonding of two adjacent **1*ox*** molecules, with an F···H distance of 2.915 (9) Å, was observed between the *m*-F atom of the polyfluoroaryl ring and a methyl H of the Et group (–$NEt_2$), the one not showing the agostic interactions with Pt (Fig. 7). These supramolecular interactions may facilitate the docking of the drug and reinforce the nucleobase–Pt interactions.

## 4. Conclusion

Further examination of the products of the reaction between [$PtCl_2\{H_2N(CH_2)_2NEt_2\}$], $Tl_2CO_3$ and bromopentafluorobenzene in refluxing pyridine has revealed that, in addition to the major product, [Pt{(*p*-$BrC_6F_4$)N$(CH_2)_2NEt_2$}Cl(py)], *i.e.* **1*p***, a significant amount of the *ortho*-stereoisomer, [Pt{(*o*-$BrC_6F_4$)N$(CH_2)_2NEt_2$}Cl(py)], *i.e.* **1*o***, can also be isolated, taking advantage of the much higher solubility of **1*o***. The new regioisomer, which was characterized by synchrotron X-ray crystallography, crystallizes as a 1:1 mixture of two rotameric isomers, *i.e.* **1*ox*** and **1*oy***, according to whether the Br substituent and the Cl ligand are in an *anti* (in **1*ox***) or *syn* (in **1*oy***) disposition. The $^1$H and $^{19}$F NMR spectra in $(CD_3)_2CO$ are consistent with the structural assignment.

## Acknowledgements

AMB gratefully acknowledges financial support from the Australian Research Council. RO thanks the Australian Government for the provision of an Australian Postgraduate Award. All the authors thank Dr Craig M. Forsyth for his help in the refinement of the crystal data. X-ray crystallography data collection in this research was undertaken on the MX1 beamline at the Australian Synchrotron, which is a part of ANSTO (Cowieson *et al.*, 2015). Open access publishing facilitated by Monash University, as part of the Wiley–Monash University agreement via the Council of Australian University Librarians.

## Funding information

Funding for this research was provided by: Australian Research Council (grant No. DP120101470).

## References

Ando, S. & Matsuura, T. (1995). *Magn. Reson. Chem.* **33**, 639–645.
Ault, J. L., Harries, H. J. & Burgess, J. (1977). *Inorg. Chim. Acta* **25**, 65–69.
Battle, A. R., Bond, A. M., Chow, A., Daniels, D. P., Deacon, G. B., Hambley, T. W., Junk, P. C., Mason, D. N. & Wang, J. (2010). *J. Fluor. Chem.* **131**, 1229–1236.
Bruce, M. I. (1968). *J. Chem. Soc. A* pp. 1459–1464.
Buxton, D. P., Deacon, G. B., Gatehouse, B. M., Grayson, I. L. & Black, D. S. C. (1988). *Aust. J. Chem.* **41**, 943–956.
Chambers, R. D. (2004). *Fluorine in Organic Chemistry*, pp. 122–136. Oxford: Blackwell Publishing Ltd.
Chambers, R. D., Musgrave, W. K. R., Waterhouse, J. S., Williams, D. L. H., Burdon, J., Hollyhead, W. B. & Tatlow, J. C. (1974). *J. Chem. Soc. Chem. Commun.* pp. 239–240.
Chambers, R. D., Waterhouse, J. S. & Williams, D. L. H. (1977). *J. Chem. Soc. Perkin Trans. 2*, pp. 585–588.
Cowieson, N. P., Aragao, D., Clift, M., Ericsson, D. J., Gee, C., Harrop, S. J., Mudie, N., Panjikar, S., Price, J. R., Riboldi-Tunnicliffe, A., Williamson, R. & Caradoc-Davies, T. (2015). *J. Synchrotron Rad.* **22**, 187–190.
Deacon, G. B., Gatehouse, B. M., Haubrich, S. T., Ireland, J. & Lawrenz, E. T. (1998). *Polyhedron* **17**, 791–802.
Deacon, G. B., Gatehouse, B. M. & Ireland, J. (1991). *Aust. J. Chem.* **44**, 1669–1681.
Dolomanov, O. V., Bourhis, L. J., Gildea, R. J., Howard, J. A. K. & Puschmann, H. (2009). *J. Appl. Cryst.* **42**, 339–341.
Kabsch, W. (1993). *J. Appl. Cryst.* **26**, 795–800.
McPhillips, T. M., McPhillips, S. E., Chiu, H.-J., Cohen, A. E., Deacon, A. M., Ellis, P. J., Garman, E., Gonzalez, A., Sauter, N. K., Phizackerley, R. P., Soltis, S. M. & Kuhn, P. (2002). *J. Synchrotron Rad.* **9**, 401–406.
Ojha, R., Boas, J. F., Deacon, G. B., Junk, P. C. & Bond, A. M. (2016). *J. Inorg. Biochem.* **162**, 194–200.
Ojha, R., Junk, P. C., Bond, A. M. & Deacon, G. B. (2023). *Molecules* **28**, 6402.
Ojha, R., Junk, P. C., Deacon, G. B. & Bond, A. M. (2018). *Supramol. Chem.* **30**, 418–424.
Ojha, R., Mason, D., Forsyth, C. M., Deacon, G. B., Junk, P. C. & Bond, A. M. (2021). *J. Inorg. Biochem.* **218**, 111360.
Ojha, R., Nafady, A., Shiddiky, M. J. A., Mason, D., Boas, J. F., Torriero, A. A. J., Bond, A. M., Deacon, G. B. & Junk, P. C. (2015). *ChemElectroChem* **2**, 1048–1061.
Sheldrick, G. M. (2015*a*). *Acta Cryst.* A**71**, 3–8.
Sheldrick, G. M. (2015*b*). *Acta Cryst.* C**71**, 3–8.
Talarico, T., Phillips, D. R., Deacon, G. B., Rainone, S. & Webster, L. K. (1999). *Invest. New Drugs* **17**, 1–15.

# supporting information

*Acta Cryst.* (2025). C**81**, 513-518 [https://doi.org/10.1107/S2053229625006837]

## *Syn*- and *anti*-rotamers of the *ortho*-stereoisomer [Pt{(*o*-$BrC_6F_4$)N($CH_2$)$_2$N$Et_2$}Cl(py)]

**Ruchika Ojha, Alan M. Bond, Peter C. Junk and Glen B. Deacon**

### Computing details

### *trans*-[*N*-(2-Bromo-3,4,5,6-tetrafluorophenyl)-*N*′,*N*′-diethylethane-1,2-diaminato(1-)]chloridopyridineplatinum(II)

*Crystal data*

$[PtBr_{0.1}(C_{12}H_{14}BrF_4N_2)(C_5H_5N)Cl_{0.9}]$ $[PtBr_{0.4}(C_{12}H_{14}BrF_4N_2)(C_5H_5N)Cl_{0.6}]$
$M_r$ = 1321.39
Triclinic, $P\overline{1}$
$a$ = 9.4810 (19) Å
$b$ = 14.656 (3) Å
$c$ = 15.094 (3) Å
$\alpha$ = 75.02 (3)°
$\beta$ = 74.62 (3)°
$\gamma$ = 86.28 (3)°
$V$ = 1953.5 (8) Å$^3$
$Z$ = 2
$F$(000) = 1246
$D_x$ = 2.246 Mg m$^{-3}$
Synchrotron radiation, $\lambda$ = 0.7108 Å
Cell parameters from 8572 reflections
$\theta$ = 1.4–27.9°
$\mu$ = 9.79 mm$^{-1}$
$T$ = 100 K
Prism, yellow
0.02 × 0.02 × 0.01 mm

*Data collection*

ADSC Quantum 210r diffractometer
Radiation source: Australian Synchrotron MX1
phi scans
24773 measured reflections
8572 independent reflections
6722 reflections with $I > 2\sigma(I)$
$R_{int}$ = 0.055
$\theta_{max}$ = 27.9°, $\theta_{min}$ = 1.4°
$h$ = −12→12
$k$ = −19→19
$l$ = −19→19
8572 standard reflections every 0 reflections
intensity decay: none

*Refinement*

Refinement on $F^2$
Least-squares matrix: full
$R[F^2 > 2\sigma(F^2)]$ = 0.063
$wR(F^2)$ = 0.174
$S$ = 1.05
8572 reflections
506 parameters
38 restraints
Primary atom site location: dual
Hydrogen site location: inferred from neighbouring sites
H-atom parameters constrained
$w = 1/[\sigma^2(F_o^2) + (0.0879P)^2 + 22.6555P]$ where $P = (F_o^2 + 2F_c^2)/3$
$(\Delta/\sigma)_{max}$ = 0.001
$\Delta\rho_{max}$ = 2.78 e Å$^{-3}$
$\Delta\rho_{min}$ = −2.37 e Å$^{-3}$
Extinction correction: SHELXL2018 (Sheldrick, 2015*b*), $Fc^*=kFc[1+0.001xFc^2\lambda^3/\sin(2\theta)]^{-1/4}$
Extinction coefficient: 0.0085 (5)

*Special details*

**Geometry**. All e.s.d.'s (except the e.s.d. in the dihedral angle between two l.s. planes) are estimated using the full covariance matrix. The cell e.s.d.'s are taken into account individually in the estimation of e.s.d.'s in distances, angles and torsion angles; correlations between e.s.d.'s in cell parameters are only used when they are defined by crystal symmetry. An approximate (isotropic) treatment of cell e.s.d.'s is used for estimating e.s.d.'s involving l.s. planes.

*Fractional atomic coordinates and isotropic or equivalent isotropic displacement parameters (Å²)*

| | *x* | *y* | *z* | $U_{iso}$*/$U_{eq}$ | Occ. (<1) |
|---|---|---|---|---|---|
| Pt1 | 0.68588 (5) | 0.26255 (3) | 0.69629 (3) | 0.03652 (16) | |
| Pt2 | 0.84692 (4) | 0.40034 (3) | 0.21031 (3) | 0.03580 (16) | |
| Br1 | 0.29324 (18) | 0.10436 (12) | 0.96603 (11) | 0.0617 (4) | |
| Br2 | 0.76261 (16) | 0.27209 (12) | 0.07351 (11) | 0.0582 (4) | |
| Br1A | 0.844 (2) | 0.4020 (10) | 0.5902 (13) | 0.036 (2) | 0.414 (11) |
| Br2A | 1.011 (5) | 0.549 (2) | 0.112 (3) | 0.0371 (12) | 0.091 (10) |
| F1 | 0.1118 (10) | −0.0192 (6) | 0.9139 (9) | 0.083 (3) | |
| F2 | 0.1215 (11) | −0.0589 (5) | 0.7548 (8) | 0.085 (3) | |
| F3 | 0.3670 (13) | 0.0166 (6) | 0.5945 (8) | 0.078 (3) | |
| F4 | 0.5838 (7) | 0.1069 (5) | 0.6057 (5) | 0.0454 (17) | |
| F5 | 0.5008 (10) | 0.1702 (7) | 0.0865 (6) | 0.065 (2) | |
| F6 | 0.2804 (7) | 0.0882 (4) | 0.2309 (6) | 0.0478 (18) | |
| F7 | 0.2840 (9) | 0.1086 (6) | 0.4125 (6) | 0.062 (2) | |
| F8 | 0.4821 (8) | 0.2093 (5) | 0.4402 (5) | 0.0447 (16) | |
| N1 | 0.5650 (12) | 0.1575 (8) | 0.7918 (8) | 0.048 (3) | |
| N2 | 0.8564 (11) | 0.1972 (7) | 0.7524 (7) | 0.040 (2) | |
| N3 | 0.5077 (10) | 0.3228 (7) | 0.6537 (7) | 0.036 (2) | |
| N4 | 0.7279 (12) | 0.2856 (8) | 0.2896 (8) | 0.048 (3) | |
| N5 | 1.0108 (10) | 0.3299 (7) | 0.2689 (8) | 0.041 (2) | |
| N6 | 0.6742 (10) | 0.4682 (7) | 0.1676 (7) | 0.0348 (19) | |
| C1 | 0.3369 (12) | 0.0695 (9) | 0.8536 (10) | 0.049 (3) | |
| C2 | 0.2294 (14) | 0.0143 (8) | 0.8452 (10) | 0.058 (4) | |
| C3 | 0.2381 (17) | −0.0042 (10) | 0.7587 (10) | 0.072 (5) | |
| C4 | 0.3514 (14) | 0.0330 (10) | 0.6810 (12) | 0.072 (5) | |
| C5 | 0.4619 (16) | 0.0853 (9) | 0.6918 (10) | 0.052 (3) | |
| C6 | 0.4588 (12) | 0.1060 (8) | 0.7783 (8) | 0.041 (3) | |
| C7 | 0.6381 (14) | 0.1128 (10) | 0.8651 (9) | 0.048 (3) | |
| H7A | 0.593910 | 0.050255 | 0.900527 | 0.057* | |
| H7B | 0.629319 | 0.152434 | 0.910403 | 0.057* | |
| C8 | 0.7960 (14) | 0.1022 (9) | 0.8160 (10) | 0.047 (3) | |
| H8A | 0.804889 | 0.055707 | 0.777419 | 0.056* | |
| H8B | 0.852798 | 0.078673 | 0.863654 | 0.056* | |
| C9 | 0.8925 (15) | 0.2589 (10) | 0.8095 (10) | 0.047 (3) | |
| H9A | 0.801059 | 0.270905 | 0.854930 | 0.056* | |
| H9B | 0.928483 | 0.320540 | 0.765718 | 0.056* | |
| C10 | 1.0060 (16) | 0.2195 (10) | 0.8650 (11) | 0.054 (3) | |
| H10A | 1.095621 | 0.203945 | 0.821542 | 0.082* | |
| H10B | 0.967023 | 0.162426 | 0.914066 | 0.082* | |
| H10C | 1.028032 | 0.266938 | 0.894813 | 0.082* | |

| | | | | |
|---|---|---|---|---|
| C11 | 0.9930 (14) | 0.1841 (10) | 0.6768 (10) | 0.048 (3) |
| H11A | 1.037998 | 0.246810 | 0.643044 | 0.058* |
| H11B | 1.064064 | 0.145908 | 0.708542 | 0.058* |
| C12 | 0.9669 (17) | 0.1370 (11) | 0.6047 (10) | 0.056 (3) |
| H12A | 1.057406 | 0.138283 | 0.554506 | 0.084* |
| H12B | 0.889970 | 0.170742 | 0.576982 | 0.084* |
| H12C | 0.936461 | 0.071332 | 0.635813 | 0.084* |
| C13 | 0.3853 (12) | 0.3349 (8) | 0.7196 (8) | 0.037 (2) |
| H13 | 0.383238 | 0.312461 | 0.784832 | 0.044* |
| C14 | 0.2652 (13) | 0.3781 (9) | 0.6955 (9) | 0.043 (3) |
| H14 | 0.180904 | 0.386731 | 0.743289 | 0.051* |
| C15 | 0.2668 (14) | 0.4097 (9) | 0.5995 (9) | 0.045 (3) |
| H15 | 0.183628 | 0.439585 | 0.580795 | 0.054* |
| C16 | 0.3898 (13) | 0.3966 (10) | 0.5339 (10) | 0.046 (3) |
| H16 | 0.393144 | 0.417337 | 0.468304 | 0.055* |
| C17 | 0.5108 (13) | 0.3533 (9) | 0.5618 (8) | 0.039 (2) |
| H17 | 0.596855 | 0.345227 | 0.515042 | 0.047* |
| C18 | 0.5011 (11) | 0.1986 (8) | 0.3484 (9) | 0.041 (3) |
| C19 | 0.3930 (14) | 0.1453 (10) | 0.3386 (9) | 0.052 (3) |
| C20 | 0.3927 (14) | 0.1386 (9) | 0.2490 (9) | 0.056 (4) |
| C21 | 0.5055 (12) | 0.1814 (9) | 0.1724 (9) | 0.049 (3) |
| C22 | 0.6140 (14) | 0.2328 (10) | 0.1837 (9) | 0.048 (3) |
| C23 | 0.6197 (12) | 0.2407 (9) | 0.2731 (7) | 0.040 (3) |
| C24 | 0.7917 (13) | 0.2382 (9) | 0.3686 (9) | 0.042 (3) |
| H24A | 0.750692 | 0.173742 | 0.398470 | 0.050* |
| H24B | 0.771736 | 0.274514 | 0.417514 | 0.050* |
| C25 | 0.9527 (13) | 0.2342 (9) | 0.3248 (9) | 0.044 (3) |
| H25A | 1.004040 | 0.209574 | 0.375300 | 0.053* |
| H25B | 0.971497 | 0.190623 | 0.282661 | 0.053* |
| C26 | 1.0383 (14) | 0.3876 (9) | 0.3331 (9) | 0.044 (3) |
| H26A | 0.944977 | 0.392396 | 0.380404 | 0.053* |
| H26B | 1.066652 | 0.452355 | 0.294031 | 0.053* |
| C27 | 1.1553 (16) | 0.3502 (11) | 0.3865 (11) | 0.056 (4) |
| H27A | 1.251437 | 0.354006 | 0.340966 | 0.084* |
| H27B | 1.133435 | 0.284230 | 0.421567 | 0.084* |
| H27C | 1.155826 | 0.388277 | 0.431002 | 0.084* |
| C28 | 1.1543 (13) | 0.3234 (10) | 0.1954 (10) | 0.044 (3) |
| H28A | 1.222347 | 0.281796 | 0.227181 | 0.053* |
| H28B | 1.199440 | 0.386960 | 0.168609 | 0.053* |
| C29 | 1.1344 (14) | 0.2848 (10) | 0.1138 (10) | 0.050 (3) |
| H29A | 1.093553 | 0.334224 | 0.070248 | 0.075* |
| H29B | 1.067544 | 0.230496 | 0.139831 | 0.075* |
| H29C | 1.229399 | 0.264957 | 0.079482 | 0.075* |
| C30 | 0.5450 (12) | 0.4683 (9) | 0.2321 (8) | 0.039 (2) |
| H30 | 0.536734 | 0.433241 | 0.295741 | 0.047* |
| C31 | 0.4239 (13) | 0.5171 (8) | 0.2102 (9) | 0.041 (3) |
| H31 | 0.334751 | 0.515894 | 0.257648 | 0.050* |
| C32 | 0.4356 (13) | 0.5677 (9) | 0.1176 (10) | 0.045 (3) |

| | | | | | |
|---|---|---|---|---|---|
| H32 | 0.354726 | 0.602666 | 0.100600 | 0.055* | |
| C33 | 0.5671 (13) | 0.5669 (9) | 0.0493 (9) | 0.043 (3) | |
| H33 | 0.575966 | 0.599672 | −0.015072 | 0.051* | |
| C34 | 0.6869 (14) | 0.5168 (9) | 0.0768 (9) | 0.044 (3) | |
| H34 | 0.777604 | 0.517330 | 0.030862 | 0.053* | |
| Cl1 | 0.837 (3) | 0.3837 (16) | 0.586 (2) | 0.030 (3) | 0.586 (11) |
| Cl2 | 0.9986 (9) | 0.5287 (5) | 0.1236 (6) | 0.0371 (12) | 0.909 (10) |

*Atomic displacement parameters (Å²)*

| | $U^{11}$ | $U^{22}$ | $U^{33}$ | $U^{12}$ | $U^{13}$ | $U^{23}$ |
|---|---|---|---|---|---|---|
| Pt1 | 0.0295 (2) | 0.0424 (3) | 0.0387 (3) | 0.00454 (19) | −0.01210 (17) | −0.00950 (18) |
| Pt2 | 0.0266 (2) | 0.0453 (3) | 0.0386 (3) | 0.00293 (19) | −0.01070 (16) | −0.01434 (19) |
| Br1 | 0.0605 (9) | 0.0669 (9) | 0.0567 (8) | −0.0041 (7) | −0.0199 (7) | −0.0080 (7) |
| Br2 | 0.0504 (8) | 0.0756 (10) | 0.0541 (8) | 0.0061 (7) | −0.0173 (6) | −0.0233 (7) |
| Br1A | 0.041 (3) | 0.030 (6) | 0.044 (2) | 0.006 (4) | −0.0188 (18) | −0.014 (3) |
| Br2A | 0.031 (2) | 0.037 (3) | 0.042 (3) | −0.002 (2) | −0.0059 (18) | −0.010 (3) |
| F1 | 0.050 (5) | 0.052 (5) | 0.127 (9) | −0.010 (4) | −0.006 (5) | 0.000 (5) |
| F3 | 0.115 (9) | 0.053 (5) | 0.092 (7) | 0.015 (5) | −0.056 (7) | −0.036 (5) |
| F5 | 0.072 (6) | 0.079 (6) | 0.068 (6) | 0.017 (5) | −0.039 (5) | −0.041 (5) |
| F6 | 0.029 (3) | 0.026 (3) | 0.093 (6) | −0.001 (3) | −0.026 (3) | −0.013 (3) |
| F7 | 0.052 (5) | 0.056 (5) | 0.070 (6) | −0.007 (4) | −0.017 (4) | 0.000 (4) |
| F8 | 0.051 (4) | 0.044 (4) | 0.043 (4) | 0.003 (3) | −0.017 (3) | −0.014 (3) |
| N1 | 0.040 (6) | 0.057 (6) | 0.046 (6) | 0.002 (5) | −0.019 (5) | −0.003 (5) |
| N2 | 0.035 (5) | 0.038 (5) | 0.049 (6) | 0.009 (4) | −0.018 (4) | −0.009 (4) |
| N3 | 0.029 (5) | 0.035 (5) | 0.046 (5) | 0.008 (4) | −0.013 (4) | −0.013 (4) |
| N4 | 0.038 (6) | 0.060 (7) | 0.049 (6) | −0.001 (5) | −0.022 (5) | −0.008 (5) |
| N5 | 0.026 (5) | 0.048 (6) | 0.055 (6) | 0.014 (4) | −0.021 (4) | −0.018 (5) |
| N6 | 0.025 (4) | 0.039 (5) | 0.042 (5) | 0.005 (4) | −0.007 (4) | −0.015 (4) |
| C1 | 0.038 (7) | 0.040 (6) | 0.065 (9) | 0.010 (6) | −0.004 (6) | −0.019 (6) |
| C2 | 0.032 (7) | 0.026 (6) | 0.109 (13) | 0.000 (5) | −0.019 (7) | −0.002 (7) |
| C3 | 0.068 (11) | 0.040 (7) | 0.128 (17) | 0.004 (8) | −0.057 (11) | −0.024 (9) |
| C4 | 0.065 (11) | 0.054 (9) | 0.116 (15) | 0.020 (8) | −0.063 (11) | −0.018 (10) |
| C5 | 0.058 (9) | 0.042 (7) | 0.066 (9) | 0.010 (6) | −0.035 (7) | −0.015 (6) |
| C6 | 0.034 (6) | 0.033 (5) | 0.056 (7) | −0.002 (5) | −0.017 (5) | −0.004 (5) |
| C7 | 0.037 (6) | 0.060 (8) | 0.043 (7) | −0.007 (6) | −0.013 (5) | −0.004 (6) |
| C8 | 0.044 (7) | 0.043 (6) | 0.051 (7) | −0.006 (6) | −0.018 (6) | 0.001 (5) |
| C9 | 0.044 (7) | 0.052 (7) | 0.050 (7) | 0.005 (6) | −0.028 (6) | −0.008 (6) |
| C10 | 0.050 (8) | 0.055 (8) | 0.071 (9) | 0.017 (7) | −0.037 (7) | −0.020 (7) |
| C11 | 0.037 (7) | 0.045 (7) | 0.064 (8) | 0.011 (6) | −0.015 (6) | −0.016 (6) |
| C12 | 0.054 (8) | 0.057 (8) | 0.054 (8) | 0.030 (7) | −0.015 (6) | −0.016 (6) |
| C13 | 0.029 (5) | 0.040 (6) | 0.042 (6) | 0.006 (5) | −0.010 (4) | −0.012 (5) |
| C14 | 0.026 (5) | 0.058 (7) | 0.051 (7) | 0.007 (5) | −0.014 (5) | −0.024 (6) |
| C15 | 0.042 (7) | 0.046 (7) | 0.054 (7) | 0.003 (6) | −0.023 (6) | −0.013 (6) |
| C16 | 0.030 (6) | 0.064 (8) | 0.052 (7) | 0.012 (6) | −0.019 (5) | −0.023 (6) |
| C17 | 0.032 (6) | 0.054 (7) | 0.033 (6) | 0.011 (5) | −0.011 (4) | −0.014 (5) |
| C18 | 0.029 (6) | 0.038 (6) | 0.058 (7) | 0.003 (5) | −0.011 (5) | −0.015 (5) |
| C19 | 0.037 (7) | 0.053 (8) | 0.066 (9) | −0.004 (6) | −0.018 (6) | −0.008 (6) |

| | | | | | | |
|---|---|---|---|---|---|---|
| C20 | 0.050 (8) | 0.040 (7) | 0.097 (12) | 0.011 (6) | −0.042 (8) | −0.031 (7) |
| C21 | 0.057 (8) | 0.054 (7) | 0.057 (8) | 0.026 (7) | −0.036 (7) | −0.033 (7) |
| C22 | 0.042 (7) | 0.058 (8) | 0.055 (8) | 0.007 (6) | −0.020 (6) | −0.027 (6) |
| C23 | 0.025 (5) | 0.047 (6) | 0.051 (7) | 0.012 (5) | −0.012 (5) | −0.016 (5) |
| C24 | 0.030 (6) | 0.052 (7) | 0.042 (6) | 0.006 (5) | −0.008 (5) | −0.015 (5) |
| C25 | 0.039 (6) | 0.050 (7) | 0.049 (7) | 0.002 (6) | −0.022 (5) | −0.011 (6) |
| C26 | 0.041 (7) | 0.053 (7) | 0.049 (7) | 0.003 (6) | −0.022 (5) | −0.021 (6) |
| C27 | 0.057 (8) | 0.058 (8) | 0.058 (8) | −0.010 (7) | −0.032 (7) | −0.004 (7) |
| C28 | 0.026 (5) | 0.050 (7) | 0.060 (8) | 0.018 (5) | −0.010 (5) | −0.023 (6) |
| C29 | 0.036 (6) | 0.058 (8) | 0.055 (8) | −0.003 (6) | −0.007 (5) | −0.018 (6) |
| C30 | 0.026 (5) | 0.053 (7) | 0.039 (6) | 0.005 (5) | −0.005 (4) | −0.018 (5) |
| C31 | 0.028 (6) | 0.041 (6) | 0.058 (7) | 0.009 (5) | −0.012 (5) | −0.018 (5) |
| C32 | 0.031 (6) | 0.050 (7) | 0.065 (8) | 0.009 (6) | −0.024 (5) | −0.020 (6) |
| C33 | 0.039 (6) | 0.043 (6) | 0.049 (7) | 0.003 (5) | −0.021 (5) | −0.007 (5) |
| C34 | 0.033 (6) | 0.054 (7) | 0.043 (6) | 0.005 (6) | −0.017 (5) | −0.002 (5) |
| Cl1 | 0.034 (4) | 0.020 (6) | 0.042 (4) | 0.001 (4) | −0.012 (3) | −0.014 (4) |
| F4 | 0.028 (3) | 0.043 (4) | 0.052 (4) | −0.001 (3) | −0.015 (3) | 0.017 (3) |
| F2 | 0.092 (7) | 0.032 (4) | 0.177 (10) | 0.015 (4) | −0.103 (7) | −0.042 (5) |
| Cl2 | 0.031 (2) | 0.037 (3) | 0.042 (3) | −0.002 (2) | −0.0059 (18) | −0.010 (3) |

*Geometric parameters (Å, º)*

| | | | |
|---|---|---|---|
| Pt1—N1 | 1.993 (11) | C10—H10B | 0.9800 |
| Pt1—N3 | 2.034 (9) | C10—H10C | 0.9800 |
| Pt1—N2 | 2.087 (10) | C11—C12 | 1.508 (19) |
| Pt1—Cl1 | 2.35 (3) | C11—H11A | 0.9900 |
| Pt1—Br1A | 2.534 (16) | C11—H11B | 0.9900 |
| Pt2—N4 | 2.006 (11) | C12—H12A | 0.9800 |
| Pt2—N6 | 2.026 (9) | C12—H12B | 0.9800 |
| Pt2—N5 | 2.076 (9) | C12—H12C | 0.9800 |
| Pt2—Cl2 | 2.323 (7) | C13—C14 | 1.355 (16) |
| Pt2—Br2A | 2.62 (3) | C13—H13 | 0.9500 |
| Br1—C1 | 1.833 (13) | C14—C15 | 1.399 (18) |
| Br2—C22 | 1.858 (14) | C14—H14 | 0.9500 |
| F1—C2 | 1.324 (16) | C15—C16 | 1.354 (18) |
| F3—C4 | 1.36 (2) | C15—H15 | 0.9500 |
| F5—C21 | 1.360 (13) | C16—C17 | 1.386 (16) |
| F6—C20 | 1.454 (13) | C16—H16 | 0.9500 |
| F7—C19 | 1.324 (15) | C17—H17 | 0.9500 |
| F8—C18 | 1.396 (14) | C18—C19 | 1.388 (11) |
| N1—C6 | 1.382 (15) | C18—C23 | 1.409 (11) |
| N1—C7 | 1.452 (15) | C19—C20 | 1.381 (12) |
| N2—C9 | 1.510 (16) | C20—C21 | 1.390 (12) |
| N2—C8 | 1.519 (15) | C21—C22 | 1.383 (11) |
| N2—C11 | 1.521 (17) | C22—C23 | 1.400 (12) |
| N3—C17 | 1.336 (14) | C24—C25 | 1.498 (17) |
| N3—C13 | 1.349 (14) | C24—H24A | 0.9900 |
| N4—C23 | 1.361 (15) | C24—H24B | 0.9900 |

| | | | |
|---|---|---|---|
| N4—C24 | 1.474 (15) | C25—H25A | 0.9900 |
| N5—C25 | 1.491 (16) | C25—H25B | 0.9900 |
| N5—C26 | 1.518 (14) | C26—C27 | 1.532 (17) |
| N5—C28 | 1.526 (15) | C26—H26A | 0.9900 |
| N6—C34 | 1.348 (15) | C26—H26B | 0.9900 |
| N6—C30 | 1.349 (14) | C27—H27A | 0.9800 |
| C1—C2 | 1.392 (12) | C27—H27B | 0.9800 |
| C1—C6 | 1.408 (12) | C27—H27C | 0.9800 |
| C2—C3 | 1.381 (13) | C28—C29 | 1.539 (18) |
| C3—C4 | 1.380 (14) | C28—H28A | 0.9900 |
| C3—F2 | 1.430 (15) | C28—H28B | 0.9900 |
| C4—C5 | 1.403 (12) | C29—H29A | 0.9800 |
| C5—C6 | 1.408 (12) | C29—H29B | 0.9800 |
| C5—F4 | 1.471 (16) | C29—H29C | 0.9800 |
| C7—C8 | 1.502 (18) | C30—C31 | 1.382 (16) |
| C7—H7A | 0.9900 | C30—H30 | 0.9500 |
| C7—H7B | 0.9900 | C31—C32 | 1.381 (19) |
| C8—H8A | 0.9900 | C31—H31 | 0.9500 |
| C8—H8B | 0.9900 | C32—C33 | 1.393 (18) |
| C9—C10 | 1.530 (16) | C32—H32 | 0.9500 |
| C9—H9A | 0.9900 | C33—C34 | 1.408 (16) |
| C9—H9B | 0.9900 | C33—H33 | 0.9500 |
| C10—H10A | 0.9800 | C34—H34 | 0.9500 |

| | | | |
|---|---|---|---|
| N1—Pt1—N3 | 91.6 (4) | H11A—C11—H11B | 107.6 |
| N1—Pt1—N2 | 84.2 (4) | C11—C12—H12A | 109.5 |
| N3—Pt1—N2 | 174.8 (4) | C11—C12—H12B | 109.5 |
| N1—Pt1—Cl1 | 177.5 (9) | H12A—C12—H12B | 109.5 |
| N3—Pt1—Cl1 | 90.9 (8) | C11—C12—H12C | 109.5 |
| N2—Pt1—Cl1 | 93.3 (8) | H12A—C12—H12C | 109.5 |
| N1—Pt1—Br1A | 173.7 (5) | H12B—C12—H12C | 109.5 |
| N3—Pt1—Br1A | 90.8 (5) | N3—C13—C14 | 122.0 (11) |
| N2—Pt1—Br1A | 93.0 (5) | N3—C13—H13 | 119.0 |
| Cl1—Pt1—Br1A | 5.7 (9) | C14—C13—H13 | 119.0 |
| N4—Pt2—N6 | 93.2 (4) | C13—C14—C15 | 119.2 (12) |
| N4—Pt2—N5 | 83.5 (4) | C13—C14—H14 | 120.4 |
| N6—Pt2—N5 | 173.9 (4) | C15—C14—H14 | 120.4 |
| N4—Pt2—Cl2 | 175.8 (4) | C16—C15—C14 | 118.4 (12) |
| N6—Pt2—Cl2 | 90.9 (4) | C16—C15—H15 | 120.8 |
| N5—Pt2—Cl2 | 92.3 (4) | C14—C15—H15 | 120.8 |
| N4—Pt2—Br2A | 177.2 (11) | C15—C16—C17 | 120.5 (12) |
| N6—Pt2—Br2A | 89.3 (10) | C15—C16—H16 | 119.8 |
| N5—Pt2—Br2A | 93.9 (10) | C17—C16—H16 | 119.8 |
| Cl2—Pt2—Br2A | 1.8 (12) | N3—C17—C16 | 120.7 (11) |
| C6—N1—C7 | 117.8 (11) | N3—C17—H17 | 119.7 |
| C6—N1—Pt1 | 126.9 (8) | C16—C17—H17 | 119.7 |
| C7—N1—Pt1 | 110.9 (8) | C19—C18—F8 | 114.3 (9) |
| C9—N2—C8 | 111.0 (10) | C19—C18—C23 | 124.0 (11) |

| | | | |
|---|---|---|---|
| C9—N2—C11 | 109.3 (10) | F8—C18—C23 | 121.7 (9) |
| C8—N2—C11 | 110.6 (10) | F7—C19—C20 | 120.1 (9) |
| C9—N2—Pt1 | 107.0 (7) | F7—C19—C18 | 120.6 (10) |
| C8—N2—Pt1 | 105.6 (7) | C20—C19—C18 | 119.0 (12) |
| C11—N2—Pt1 | 113.3 (8) | C19—C20—C21 | 118.6 (11) |
| C17—N3—C13 | 119.3 (10) | C19—C20—F6 | 123.1 (10) |
| C17—N3—Pt1 | 121.4 (8) | C21—C20—F6 | 118.2 (9) |
| C13—N3—Pt1 | 119.3 (8) | F5—C21—C22 | 122.8 (11) |
| C23—N4—C24 | 118.6 (11) | F5—C21—C20 | 115.7 (9) |
| C23—N4—Pt2 | 130.7 (8) | C22—C21—C20 | 121.5 (11) |
| C24—N4—Pt2 | 109.7 (7) | C21—C22—C23 | 121.8 (12) |
| C25—N5—C26 | 111.1 (10) | C21—C22—Br2 | 113.4 (8) |
| C25—N5—C28 | 111.2 (10) | C23—C22—Br2 | 124.1 (8) |
| C26—N5—C28 | 108.2 (9) | N4—C23—C22 | 124.7 (10) |
| C25—N5—Pt2 | 107.0 (7) | N4—C23—C18 | 120.6 (10) |
| C26—N5—Pt2 | 105.7 (7) | C22—C23—C18 | 114.7 (10) |
| C28—N5—Pt2 | 113.5 (8) | N4—C24—C25 | 105.2 (10) |
| C34—N6—C30 | 119.0 (10) | N4—C24—H24A | 110.7 |
| C34—N6—Pt2 | 121.6 (8) | C25—C24—H24A | 110.7 |
| C30—N6—Pt2 | 119.3 (8) | N4—C24—H24B | 110.7 |
| C2—C1—C6 | 123.3 (12) | C25—C24—H24B | 110.7 |
| C2—C1—Br1 | 113.9 (9) | H24A—C24—H24B | 108.8 |
| C6—C1—Br1 | 122.3 (8) | N5—C25—C24 | 110.7 (10) |
| F1—C2—C3 | 115.7 (11) | N5—C25—H25A | 109.5 |
| F1—C2—C1 | 124.7 (12) | C24—C25—H25A | 109.5 |
| C3—C2—C1 | 119.4 (13) | N5—C25—H25B | 109.5 |
| C4—C3—C2 | 120.2 (13) | C24—C25—H25B | 109.5 |
| C4—C3—F2 | 123.5 (11) | H25A—C25—H25B | 108.1 |
| C2—C3—F2 | 116.3 (11) | N5—C26—C27 | 116.4 (11) |
| F3—C4—C3 | 123.0 (11) | N5—C26—H26A | 108.2 |
| F3—C4—C5 | 117.4 (13) | C27—C26—H26A | 108.2 |
| C3—C4—C5 | 119.5 (15) | N5—C26—H26B | 108.2 |
| C4—C5—C6 | 122.7 (13) | C27—C26—H26B | 108.2 |
| C4—C5—F4 | 111.8 (11) | H26A—C26—H26B | 107.3 |
| C6—C5—F4 | 125.3 (10) | C26—C27—H27A | 109.5 |
| N1—C6—C5 | 124.5 (10) | C26—C27—H27B | 109.5 |
| N1—C6—C1 | 120.6 (10) | H27A—C27—H27B | 109.5 |
| C5—C6—C1 | 114.8 (11) | C26—C27—H27C | 109.5 |
| N1—C7—C8 | 106.9 (11) | H27A—C27—H27C | 109.5 |
| N1—C7—H7A | 110.3 | H27B—C27—H27C | 109.5 |
| C8—C7—H7A | 110.3 | N5—C28—C29 | 113.1 (10) |
| N1—C7—H7B | 110.3 | N5—C28—H28A | 109.0 |
| C8—C7—H7B | 110.3 | C29—C28—H28A | 109.0 |
| H7A—C7—H7B | 108.6 | N5—C28—H28B | 109.0 |
| C7—C8—N2 | 109.4 (11) | C29—C28—H28B | 109.0 |
| C7—C8—H8A | 109.8 | H28A—C28—H28B | 107.8 |
| N2—C8—H8A | 109.8 | C28—C29—H29A | 109.5 |
| C7—C8—H8B | 109.8 | C28—C29—H29B | 109.5 |

| | | | |
|---|---|---|---|
| N2—C8—H8B | 109.8 | H29A—C29—H29B | 109.5 |
| H8A—C8—H8B | 108.2 | C28—C29—H29C | 109.5 |
| N2—C9—C10 | 115.8 (11) | H29A—C29—H29C | 109.5 |
| N2—C9—H9A | 108.3 | H29B—C29—H29C | 109.5 |
| C10—C9—H9A | 108.3 | N6—C30—C31 | 123.1 (11) |
| N2—C9—H9B | 108.3 | N6—C30—H30 | 118.4 |
| C10—C9—H9B | 108.3 | C31—C30—H30 | 118.4 |
| H9A—C9—H9B | 107.4 | C32—C31—C30 | 118.4 (12) |
| C9—C10—H10A | 109.5 | C32—C31—H31 | 120.8 |
| C9—C10—H10B | 109.5 | C30—C31—H31 | 120.8 |
| H10A—C10—H10B | 109.5 | C31—C32—C33 | 119.4 (11) |
| C9—C10—H10C | 109.5 | C31—C32—H32 | 120.3 |
| H10A—C10—H10C | 109.5 | C33—C32—H32 | 120.3 |
| H10B—C10—H10C | 109.5 | C32—C33—C34 | 119.2 (12) |
| C12—C11—N2 | 114.6 (11) | C32—C33—H33 | 120.4 |
| C12—C11—H11A | 108.6 | C34—C33—H33 | 120.4 |
| N2—C11—H11A | 108.6 | N6—C34—C33 | 120.8 (12) |
| C12—C11—H11B | 108.6 | N6—C34—H34 | 119.6 |
| N2—C11—H11B | 108.6 | C33—C34—H34 | 119.6 |

| | | | |
|---|---|---|---|
| C6—C1—C2—F1 | −178.4 (13) | F8—C18—C19—F7 | −0.5 (19) |
| Br1—C1—C2—F1 | −6.4 (18) | C23—C18—C19—F7 | −179.5 (12) |
| C6—C1—C2—C3 | −2 (2) | F8—C18—C19—C20 | 173.3 (11) |
| Br1—C1—C2—C3 | 169.9 (11) | C23—C18—C19—C20 | −6 (2) |
| F1—C2—C3—C4 | 175.8 (14) | F7—C19—C20—C21 | 177.3 (13) |
| C1—C2—C3—C4 | −1 (2) | C18—C19—C20—C21 | 3 (2) |
| F1—C2—C3—F2 | −1.5 (19) | F7—C19—C20—F6 | −3 (2) |
| C1—C2—C3—F2 | −178.1 (12) | C18—C19—C20—F6 | −177.0 (12) |
| C2—C3—C4—F3 | 179.2 (13) | C19—C20—C21—F5 | 178.4 (11) |
| F2—C3—C4—F3 | −4 (2) | F6—C20—C21—F5 | −1.1 (17) |
| C2—C3—C4—C5 | 3 (2) | C19—C20—C21—C22 | −2 (2) |
| F2—C3—C4—C5 | −179.5 (13) | F6—C20—C21—C22 | 178.2 (11) |
| F3—C4—C5—C6 | −179.3 (12) | F5—C21—C22—C23 | −177.7 (12) |
| C3—C4—C5—C6 | −3 (2) | C20—C21—C22—C23 | 3 (2) |
| F3—C4—C5—F4 | −4.5 (18) | F5—C21—C22—Br2 | −6.9 (17) |
| C3—C4—C5—F4 | 171.5 (13) | C20—C21—C22—Br2 | 173.8 (11) |
| C7—N1—C6—C5 | −122.4 (14) | C24—N4—C23—C22 | −133.8 (13) |
| Pt1—N1—C6—C5 | 31.8 (18) | Pt2—N4—C23—C22 | 34.1 (19) |
| C7—N1—C6—C1 | 57.3 (17) | C24—N4—C23—C18 | 47.0 (17) |
| Pt1—N1—C6—C1 | −148.4 (11) | Pt2—N4—C23—C18 | −145.1 (11) |
| C4—C5—C6—N1 | −179.7 (13) | C21—C22—C23—N4 | 176.1 (13) |
| F4—C5—C6—N1 | 6 (2) | Br2—C22—C23—N4 | 6.3 (19) |
| C4—C5—C6—C1 | 0.5 (19) | C21—C22—C23—C18 | −4.7 (19) |
| F4—C5—C6—C1 | −173.6 (12) | Br2—C22—C23—C18 | −174.4 (10) |
| C2—C1—C6—N1 | −177.5 (12) | C19—C18—C23—N4 | −174.7 (13) |
| Br1—C1—C6—N1 | 11.1 (18) | F8—C18—C23—N4 | 6.4 (19) |
| C2—C1—C6—C5 | 2.2 (19) | C19—C18—C23—C22 | 6.1 (19) |
| Br1—C1—C6—C5 | −169.2 (10) | F8—C18—C23—C22 | −172.8 (11) |

| | | | |
|---|---|---|---|
| C6—N1—C7—C8 | 115.2 (12) | C23—N4—C24—C25 | 124.3 (12) |
| Pt1—N1—C7—C8 | −43.0 (13) | Pt2—N4—C24—C25 | −46.0 (11) |
| N1—C7—C8—N2 | 53.0 (14) | C26—N5—C25—C24 | 81.0 (11) |
| C9—N2—C8—C7 | 78.8 (12) | C28—N5—C25—C24 | −158.4 (9) |
| C11—N2—C8—C7 | −159.7 (10) | Pt2—N5—C25—C24 | −33.9 (11) |
| Pt1—N2—C8—C7 | −36.8 (11) | N4—C24—C25—N5 | 52.8 (13) |
| C8—N2—C9—C10 | 59.8 (15) | C25—N5—C26—C27 | 63.8 (14) |
| C11—N2—C9—C10 | −62.5 (14) | C28—N5—C26—C27 | −58.5 (14) |
| Pt1—N2—C9—C10 | 174.5 (10) | Pt2—N5—C26—C27 | 179.5 (10) |
| C9—N2—C11—C12 | −170.6 (11) | C25—N5—C28—C29 | 69.7 (13) |
| C8—N2—C11—C12 | 66.9 (13) | C26—N5—C28—C29 | −168.0 (11) |
| Pt1—N2—C11—C12 | −51.4 (13) | Pt2—N5—C28—C29 | −51.0 (13) |
| C17—N3—C13—C14 | −0.7 (17) | C34—N6—C30—C31 | −0.8 (17) |
| Pt1—N3—C13—C14 | 177.2 (9) | Pt2—N6—C30—C31 | 176.3 (9) |
| N3—C13—C14—C15 | 1.1 (18) | N6—C30—C31—C32 | 0.4 (18) |
| C13—C14—C15—C16 | −0.6 (19) | C30—C31—C32—C33 | 1.0 (18) |
| C14—C15—C16—C17 | −0.3 (19) | C31—C32—C33—C34 | −2.0 (18) |
| C13—N3—C17—C16 | −0.3 (17) | C30—N6—C34—C33 | −0.2 (18) |
| Pt1—N3—C17—C16 | −178.1 (9) | Pt2—N6—C34—C33 | −177.3 (9) |
| C15—C16—C17—N3 | 1 (2) | C32—C33—C34—N6 | 1.6 (19) |